Dynamic Chemical Devices: Modulation of Photophysical Properties by Reversible, Ion-Triggered, and Proton-Fuelled Nanomechanical Shape-Flipping Molecular Motions

Mihail Barboiu,[a, b] Luca Prodi,[c] Marco Montalti,[c] Nelsi Zaccheroni,[c] Nathalie Kyritsakas,[d] and Jean-Marie Lehn*[a]

Abstract: The terpy-derived (terpy = terpyridine) ligand **1** has an extended W shape in which the two appended photoactive pyrenyl groups are held apart. On binding of a zinc(II) ion with a terpy group, ligand **1** is converted into complex **2** whereby it adopts a U shape, thus stacking the aromatic units. This structural modification leads to a very pronounced change in photophysical properties: from a highly fluorescent free ligand to a very weakly emitting complex. The W/U structural switching can be reversibly induced by the addition of a competitive tren ligand, which binds and releases a zinc(II) ion under protonation/deprotonation cycles, thus leading to oscillations in light emission. Therefore, the present system performs periodic modulation of optical output through a nanomechanical shape-flipping motion, triggered by metal ion binding and fuelled by acid–base neutralisation energy. Overall, it represents an ion-triggered opto-mechanical supramolecular device.

Keywords: cation binding · fluorescence · molecular devices · molecular switching · supramolecular chemistry

Introduction

The design of functional chemical devices with the potential for information storage is a major aspect of supramolecular chemistry.[1,2] Mechano-devices[2] effecting triggered molecular motions induced by light excitation, electron transfer, or ion binding provide the basis for controlled, dynamic structural changes based on rotations and translations[2] or coiling–uncoiling processes.[3] Photonic systems undergoing dynamic structural changes may be considered as encompassing two types of behaviour: 1) light-induced nanomechanical processes comprising molecular or supramolecular devices that undergo reversible changes in shape when triggered by light[1,2] allowing the reversible modulation of a given property, such as electronic conjugation,[4] and conversely, 2) effector-triggered structural (constitutional or conformational) switching of optical properties comprising devices that transform chemical processes, such as electron transfer or ion binding, into specific molecular motions, resulting in the modulation of output optical properties.[1–3]

DNA frameworks have been used in structural–optical switching processes[5a,b] and in the design of molecular beacons;[5c] however, chemistry can develop effector-triggered nanomechanical devices without resorting to molecules of biological type, thus offering higher diversity, closer structural and dynamic control as well as a more compact size.

Of special interest are photo-ionic devices undergoing reversible ionic modulation of the optical properties, such as modulation of photochemical output properties through shape changes induced by ion binding, particularly in view of their ability to couple photonic and ionic processes. As part of our studies on dynamic chemical devices,[3] we describe herein the ionic modulation of photoluminescence properties in a motional process involving reversible switching between a highly luminescent ligand **L** in a W-shaped state and its poorly luminescent metallosupramolecular U-

[a] Dr. M. Barboiu, Prof. J.-M. Lehn
Laboratoire de Chimie Supramoléculaire, ISIS
Université Louis Pasteur, 8, allée Gaspard Monge
BP 70028, 67083 Strasbourg Cedex (France)
Fax: (+33) 3-90-24-51-40
E-mail: lehn@isis.u-strasbg.fr

[b] Dr. M. Barboiu
Present address: Institut Européen des Membranes –
IEM-CNRS 5635, Place Eugène Bataillon
CC 47, 34095 Montpellier (France)

[c] Dr. L. Prodi, Dr. M. Montalti, Dr. N. Zaccheroni
Università di Bologna, Dipartimento di Chimica "G. Ciamician"
Via Selmi 2, 40126 Bologna (Italy)

[d] N. Kyritsakas
Laboratoire de Cristallochimie, Institut Le Bel
Université Louis Pasteur, 4, rue Blaise Pascal
67000 Strasbourg (France)

 DOI: 10.1002/chem.200306045

shaped complex [**LZn**], triggered by ion complexation–decomplexation reactions, as depicted in Scheme 1a.

Recent studies of related systems have involved the tuning of electronic coupling in hydroquinone-appended terpyridines by ion complexation[6] as well as tweezer-type binding processes.[7]

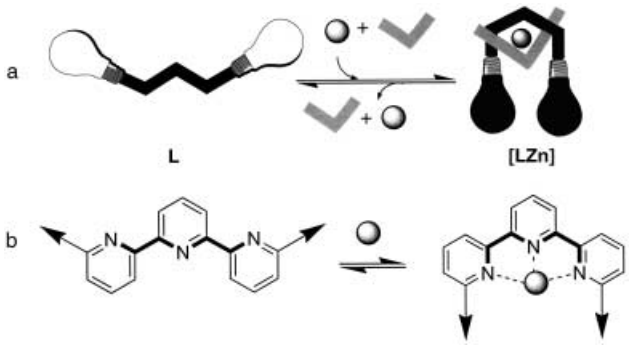

Scheme 1. Concept and design of the ion-triggered photonic supramolecular device: a) ionic modulation of the coupled fluorescence–extension/contraction structural switching processes; the angular symbol represents an additional ligand for the zinc(II) ion (shown as a sphere); b) conversion of the extended *transoid*,*transoid* form of the free terpyridine-type ligand into the compact *cisoid*,*cisoid* form of its metal complex.

Ligand design and synthesis: In view of the strongly enforced (by about 25 kJ mol^{-1})[8] *transoid* conformation about the connecting NC–CN bond in α,α′-bipyridine (bipy), extended α,α′-(py,py) sequences, such as terpyridine (terpy) units, are expected to adopt an open zigzag-type conformation, thus disposing α,α′-linked substituents at maximal distance. On the other hand, metal ion binding imposes the *cisoid* arrangement, as is common in the very numerous complexes of bipy. In the case of a terpy unit, tridentate metal ion coordination converts the W-shaped *transoid*,*transoid* form of the free ligand into the *cisoid*,*cisoid* U-shaped form corresponding to the well-known tridentate terpy-type complexation site (Scheme 1b). Specifically, the conversion of the bis terminally appended α,α′-pyrene–terpy derivative (**1**) into the corresponding Zn^{II} complex (**2**) transforms an unwrapped free ligand into a wrapped, compact coordination complex (Scheme 2) through a butterfly-type molecular motion triggered by metal ion binding. In complex **2**, the two terminal α,α′-linked π-donor pyrene units are situated in a face-to-face arrangement suitable for the insertion of a flat aromatic π-acceptor, such as a complexed terpy unit, between their parallel planes, thus yielding a compact π–π stacking subset of three overlapping aromatic rings (Scheme 1a, Scheme 2). Such a process generates a reversible conformational switching operation, which may simultaneously involve optical properties and substrate binding as a result of a specific molecular motion in an iono-mechanical supramolecular device using both appropriate metal ions and π-acceptor units. One may consider that it amounts to an optical nanodevice functioning through ion-triggered large-amplitude molecular motion.

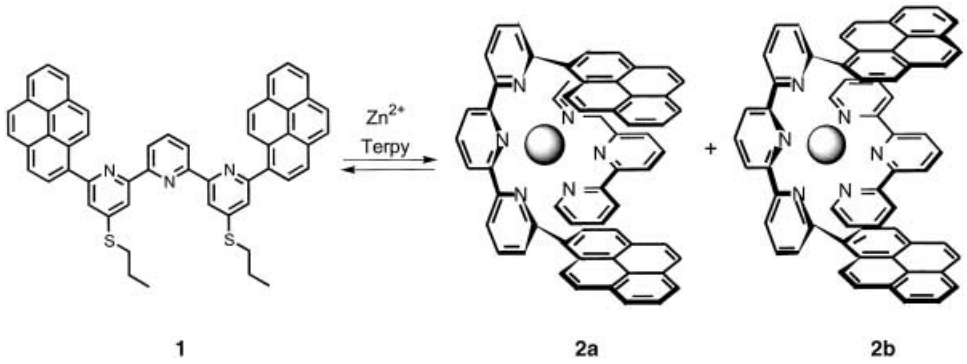

Scheme 2. Formation of complex **2** displaying the parallel- (**2a**) and antiparallel-oriented (**2b**) pyrene moieties in the complex.

Abstract in French: *Le ligand **1** dérivé de la terpyridine (terpy) présente une forme en extension W dans laquelle les deux groupes photoactifs pyrényles, greffés aux deux extrémités, sont maintenus éloignés. La complexation d'un cation Zn^{II} accompagné d'un groupe terpy conduit à un complexe **2** dans lequel le ligand adopte une forme en U, causant de ce fait un rapprochement des extrémités et un empilement des groupes aromatiques. Ce changement de structure produit une modification très prononcée des propriétés photophysiques allant d'un ligand fortement fluorescent à un complexe qui ne l'est que très faiblement. La commutation W/U peut être induite réversiblement par addition d'un agent complexant compétitif, le ligand tren, qui lie et relibère un ion Zn^{II} au cours de cycles de protonation/déprotonation, produisant de ce fait des oscillations de l'émission de lumière. Le système décrit réalise ainsi une modulation périodique du signal optique par l'effet d'un mouvement nanomécanique de changement de forme, déclenché par la fixation d'un ion métallique et dont l'énergie est fournie par la réaction de neutralisation acide/base. Il représente un dispositif supramoléculaire optomécanique à déclenchement ionique.*

Ligand **1** was synthesised by using a repetitive twofold reaction of the central pyridine bis-Michael acceptor unit **3**[9] with two 1-acetylpyrene building blocks (**4**) in a 55% yield (see Experimental Section, Scheme 3). ^{1}H NMR analysis of a solution of **1** in deuterated chloroform produced a sharp spectrum consistent with the *transoid*,*transoid* conformation of the ligand. Strong deshielding was observed for the *meta*-pyridine and the H4 pyrene hydrogen atoms indicating contact with the nitrogen pyridine atoms, in agreement with the unwrapped W conformation of compound **1**.

Crystal structure of ligand 1: Suitable crystals of **1** for X-ray structure determination were obtained by slow diffusion of acetonitrile into a solution of **1** in chloroform at room temperature. The molecular structure and packing are presented

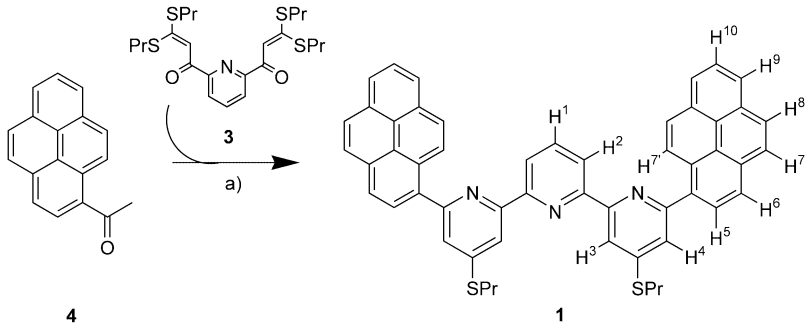

Scheme 3. Synthesis of ligand **1**: a) Compound **3**, *t*BuOK and THF at 60 °C, then NH_4OAc and AcOH at 80 °C.

in Figure 1. Ligand **1** displays an unwrapped W-shaped structure positioning the two pyrene substituents at a centroid–centroid distance of about 16.5 Å. The terpy unit exhibits a slight deviation from planarity (py-py torsional angle of about 18.6°), whereas the pyrene units are significantly rotated with respect to the terpy plane (pyridine-pyrene torsional angle of about 46.0°, Figure 1a). The relative arrangement of **1** in the crystal is very interesting and deserves some more comments. As shown in Figure 1b, the molecules of **1** are π–π-stacked in polymeric aggregates presenting tight contacts between one pyrene unit and two pyridine rings of the next terpy unit (centroid–centroid distance of 3.64 Å). Accordingly, columnar arrays of alternating stacked molecules are generated in the solid state as well as in solution (see below) by self-organisation through π-donor (pyrene) and π-acceptor (terpy) interactions.

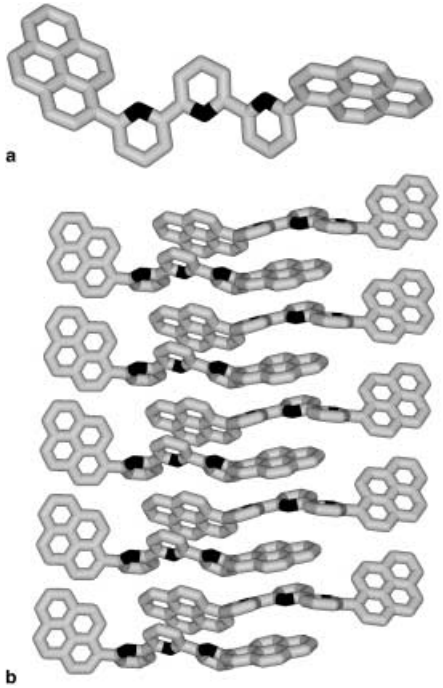

Figure 1. Crystal structure of the extended W form of the free ligand **1**: a) stick representation; b) representation of the packing of π–π-stacked polymeric aggregates; the *n*PrS substituents and hydrogen atoms have been omitted for clarity.

Photophysical properties of ligand 1: The absorption spectrum of **1** in dichloromethane is very different from that expected from a simple sum of the spectra of terpy[10] and pyrene[11] derivatives (Figure 2). In particular, the typical structured bands of pyrene at 250–280 and 310–360 nm are much broader, presenting almost no vibrational structure. In addition, the lowest energy band shows a small redshift and a tail up to 400 nm. Ligand **1** displays a large, nonstructured, very intense emission band at 408 nm in dichloromethane ($\tau =$ 2.6 ns, $\Phi = 0.33$; Figure 2 and Table 1), and properties which

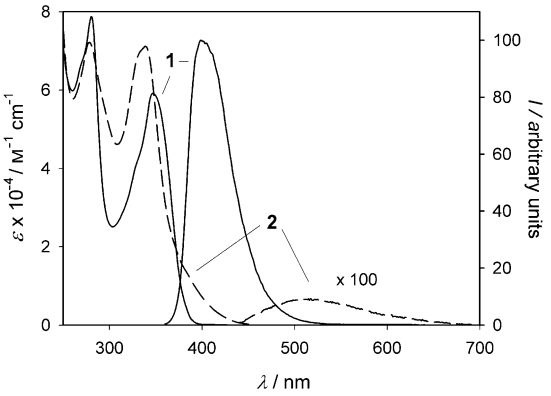

Figure 2. Absorption and fluorescence spectra ($\lambda_{exc} = 348$ nm) of ligand **1** (——) and of complex **2** (– – –) in CH_2Cl_2 at room temperature; emission intensity *I* (-----; right scale) in arbitrary units.

are almost independent of the solvent used. Corrected excitation spectra performed with λ_{em} between 380 and 500 nm are all proportional to the absorption spectrum, indicating that the emissive excited state is populated with unitary efficiency independently from the moiety of the ligand that is excited. In this case, the fluorescence band is quite different from those shown by pyrene derivatives[11], which typically display, in their monomeric form, a structured band with a much longer lifetime (>100 ns in degassed solutions). This

Table 1. Photophysical properties of ligand **1** and its complex **2** at room temperature.

	λ_{max} [nm]	ε_{max} [$M^{-1}cm^{-1}$]	λ_{max} [nm]	τ [ns]	Φ	Solvent
1	348	59200	404	2.6	0.33	CH_2Cl_2
	348	62500	401	2.6	0.34	$CHCl_3$/ CH_3CN
2	340	70200	527	<0.5	$<5\times10^{-5}$	CH_2Cl_2
	341	71100	573	<0.5	$<5\times10^{-5}$	$CHCl_3$/ CH_3CN

band differs also from that of pyrene derivatives forming excimers, since in these cases the band is even broader and centred at lower energy (typically around 480 nm). Because of the much lower Stokes shift observed in the present case and in agreement with the crystal structure results, the attribution of the observed band to an excimer-type emission, although possible in theory due to the presence of two chromophoric units, can be ruled out. Instead, the emission and the lowest energy absorption bands can be assigned to a transition mainly centred on the pyrene chromophore, with only a partial charge-transfer character involving the terpy moiety. This behaviour is slightly different from that found for a bis(bipyridyl)pyrimidine ligand substituted with an anthracene chromophore;[12] in this case, a stronger dependence on solvent polarity was found, since a redshift of the fluorescence band from 500 to 520 nm was observed on passing from dichloromethane to butyronitrile suggesting a substantial charge-transfer character for the transition responsible for the observed luminescence.

Formation and crystal structure of complex 2: Addition of $Zn(CF_3SO_3)_2$/terpy mixtures (1:1 mol/mol) to suspensions of **1** in acetonitrile caused a rapid dissolution of the ligand to give yellow solutions of the complex $[Zn(\mathbf{1})(terpy)](CF_3SO_3)_2$ (**2**). Complex **2** showed a very complicated and broad ^1H NMR spectrum at 25 °C, indicative of the presence of several exchanging species in solution. At −30 °C, the spectrum displays sharp signals for ligand **1**, located in two different magnetic environments in a 1:1 ratio, consistent with the presence of parallel- (**2a**) and antiparallel-oriented (**2b**) pyrene moieties in the complex (Scheme 2).

The molecular structure and packing of complex **2** were determined on crystals obtained from a solution of **2** in isopropyl ether/nitromethane (1:1 v/v) at room temperature (Figure 3).

Complex **2** results from the simultaneous binding of a Zn^{2+} ion and a terpy unit, with octahedral coordination of the Zn^{2+} ions (average Zn–N bonds length of 2.14 Å), and favourable π–π stacking interactions between the π-donor pyrene groups and the π-acceptor terpy unit. Ligand **1** presents a wrapped U-shaped conformation (Figure 3a) with the two pyrene moieties positioned in a face-to-face arrangement (centroid–centroid distance of about 6.90 Å). It provides a slot suitable for the intercalation of a terpy unit coordinated to the Zn^{2+} cation, leading to the formation of a π-donor–π-acceptor–π-donor triad exhibiting a considerable overlap between aromatic groups, with an average centroid–centroid distance of 3.50 Å. In the crystal, the complexes are within van der Waals contact of the anions, and the solvent molecules fill the voids between them. One may point out the role of internal stacking interactions in the cohesion, which are expected to cause a broadening of the bands of the chromophore involved, as indeed observed (see below).

Photophysical properties of complex 2: The most relevant photophysical data for complex **2** are gathered in Table 1, while the absorption spectra in dichloromethane are shown in Figure 2. Complexation with d^{10} Zn^{2+} ions does not usually introduce low-energy metal-centred or charge-transfer

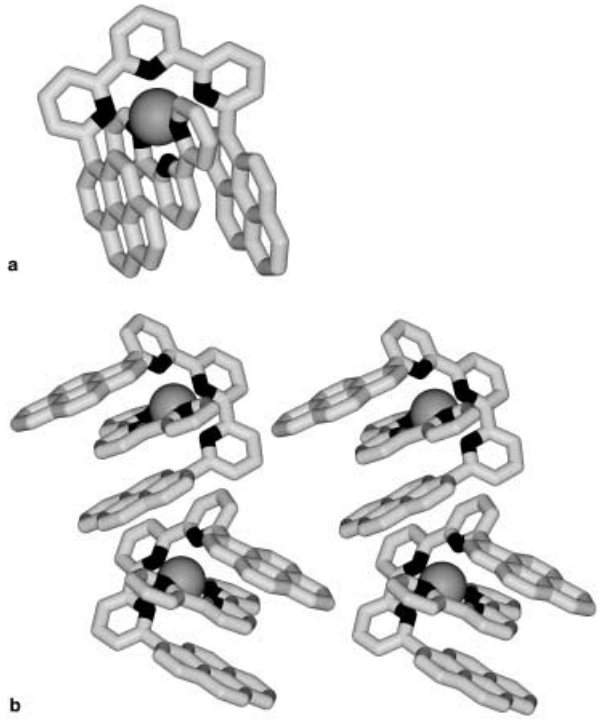

Figure 3. Crystal structure of complex **2** $[Zn^{2+}(\mathbf{1})(terpy)]$: a) stick representation; b) representation of the arrangements of the entities in the crystal; the *n*PrS substituents and hydrogen atoms have been omitted for clarity.

states into the ligand, so that MC, MLCT, or LMCT bands are not expected to be present in the absorption spectrum of Zn^{2+} complexes. As a consequence, the absorption spectrum of **2** should be regarded as the sum of the transitions involving the ligands present in the different species as perturbed by metal ion complexation[10,13] and the π–π-stacking interactions among them. The pyrene central band lying in the 320–400 nm region experiences a blueshift but with a noticeable increase of the absorption tail in the red part of the spectrum. The overall effect can be explained by taking into account two different phenomena: firstly, complexation with the metal ion decreases the electronic density on the terpy moiety, and as a consequence, perturbs the electronic structure of the pyrene unit leading to the observed blueshift of the band; secondly, this process enables the terpy unit to be more easily reduced so that a charge-transfer transition from the pyrene unit becomes possible ($E_{ox} = +1.18$ V versus SCE in acetonitrile). A charge-transfer transition was also observed in a Ru complex that had a ligand consisting of a terpy unit covalently linked to a pyrene unit.[14] Complex **2** shows a very weak ($\Phi < 5 \times 10^{-5}$), large and unstructured fluorescence band in the 480–750 nm region both in dichloromethane and acetonitrile. The excitation spectrum is also proportional to the absorption spectrum in this case.[15] In agreement with the crystal structure results above, the fluorescence band of complex **2** can be attributed, because of its shape, energy and solvent dependency, to a charge-transfer transition from the pyrene moiety to the coordinated terpy unit.

Proton-fuelled reversible modulation of photophysical properties by interconversion of ligand 1 and complex 2: We have recently shown that the motions generated by the reversible interconversions between helical ligand strands and their extended complexes, upon ion-induced contraction/extension[3a] or single/double helix[3b] dynamic processes, could be chemically controlled in a manner reminiscent of that of proteins capable of transforming physicochemical modifications into motion. These systems represent a prototype for a molecular actuator or engine type of dynamic device fuelled by ionic processes.

The transformation of the W-shaped free ligand **1** into the corresponding U-shaped form of the ligand in complex **2** offers the opportunity to set up a reversible motional process in which a molecular entity undergoes sequential nanomechanical interconversions between two states, presenting different luminescence outputs in both energy and intensity, triggered by external chemical inputs. A system that can produce reversible pulses of Zn^{2+} ions was achieved by taking advantage of the properties of the *N*,*N*-bis(2-aminoethyl)ethane-1,2-diamine (tren) ligand, which forms a strong, pH-dependent complex [Zn^{2+}(tren)] with Zn^{2+} ions.[16] From the analysis of the absorption and emission spectra taken during the titration of **1** by Zn^{2+}, a stability constant of $\log K_s = 8.0$ was obtained for the 1:1 complex in organic medium.

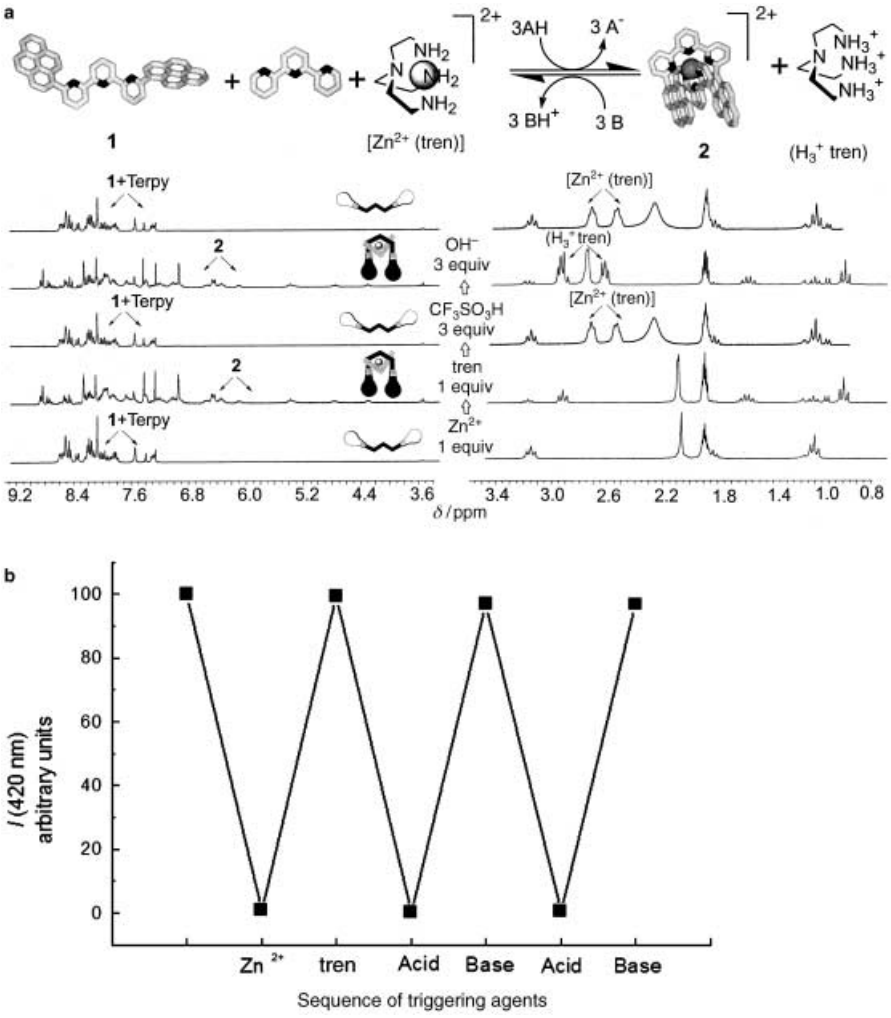

Figure 4. a) Ionic modulation of the coupled fluorescence–extension/contraction switching process, followed by the 250 MHz ^{1}H NMR spectral changes occurring on structural interconversion in the system **1**/**2** on successive addition of different triggering agents. b) Photoswitching cycles generated by ion/pH-induced iono-mechanical structural interconversion of the coupled fluorescence–extension/contraction processes.

Figure 4a shows the evolution of the aromatic and aliphatic parts of the ^{1}H NMR spectra as a function of triggering agent: Zn^{2+}, tren, CF_3SO_3H, or LiOH.

The addition of one equivalent of Zn^{2+} to a solution ($CDCl_3/CD_3CN = 1{:}1$ v/v) of free unwrapped ligand **1** and terpy (1:1 mol/mol) leads to the wrapped Zn^{2+} complex **2**. This transformation is characterised by the disappearance of the signals of ligands **1** and terpy and by the appearance of deshielded signals of both Zn^{2+}-complexed terpy units, as well as by the marked shielding of π–π-stacked pyrene and terpy hydrogen atoms. In the fluorescence spectrum, the almost complete quenching of the fluorescence of **1** can be observed.

On addition of a strong Zn^{2+} complexant, such as tren, the signals of the free ligands **1** and terpy reappear and the aliphatic part of the spectrum shows peaks that correspond to the complex [Zn^{2+}(tren)], while the typical luminescence of **1** is also restored. Lowering the pH by addition of CF_3SO_3H induces protonation of the terminal nitrogen atoms of tren causing the release of the complexed Zn^{2+} ions,[16] which then bind again to ligand **1** leading to the wrapped Zn^{2+} complex **2**. The aliphatic part of the spectrum shows the signals of protonated tren (H_3^+tren), while the aromatic-proton signals correspond to unprotonated **1**. Protonation of **1** leads to very different spectra.[17] Again, the typical fluorescence of **1** disappears. Subsequent deprotonation of the latter by addition of LiOH restores the NMR spectrum of the unwrapped form of **1** and of the complex [Zn^{2+}(tren)] in addition to the fluorescence of **1**. Repetitive interconversions of **1** and **2** can be pursued in this way by successive additions of acid and base, controlling the repetitive exchange of Zn^{2+} between **1** and the tren ligand. The interconversion is complete within the time of mixing and recording of the NMR spectra.

Since the overall centroid–centroid distance between the two pyrene moieties is about 16.5 Å in W-shaped ligand **1** and 6.90 Å in U-shaped complex **2**, the **1/2** interconversion generates a marked extension/contraction motion between two states presenting different optical output signals. The modulation of the coupled fluorescence–extension/contraction structural switching processes (Figure 4b) is induced by coupled ion-binding/protonation events and fuelled by acid–base neutralisation reactions.

Conclusion

Using a suitable molecular structural design and a simple chemical mechanism, it is possible to control, through ion binding, both molecular motions and linked modifications in optical properties.

The system described here represents a molecular actuator type of dynamic supramolecular device, displaying butterfly-like W/U extension/compression motions fuelled by ionic processes, and undergoing iono-mechanical cycles generating a periodic switching of optical properties. Such coupling of ionically triggered changes of shape and of photophysical properties also represent molecular signalisation processes involving interconversion between ionic and conformational signals and resembling biological signal transduction.

Experimental Section

General methods: All reagents were obtained from commercial suppliers and used without further purification. THF was distilled over benzophenone/Na. All organic solutions were routinely dried by using sodium sulfate (Na_2SO_4). The solvents used for the photophysical measurements were acetonitrile and dichloromethane from Merck (UVASOL). Column chromatography was carried out on Merck alumina activity II-III.^{1}H NMR, ^{13}C NMR, COSY and NOESY spectra and NMR ionic modulation experiments were recorded on a 250 MHz Bruker spectrometer with samples dissolved in $CDCl_3$ or CD_3CN, with the use of the residual solvent peak as reference. Mass spectrometric studies were performed in the positive-ion mode using a quadrupole mass spectrometer (Micromass, Platform II). Samples were dissolved in acetonitrile and were continuously introduced into the mass spectrometer through a Waters 616HPLC pump (flow rate of 10 mL min^{-1}). The temperature (60 °C) and the extraction cone voltage (V_c = 5–10 V) were usually set to avoid fragmentations. The microanalyses were carried out at Service de Microanalyses, Institut Charles Sadron, Strasbourg.

The numbering used for the assignments of the ^{1}H NMR signals (according to the corresponding COSY and ROESY spectra) for ligand **1** are given in Scheme 3.

UV/Vis absorption spectra were obtained by using a Perkin Elmer Lambda 16 spectrophotometer. Uncorrected emission and corrected excitation spectra were obtained with a Perkin Elmer LS 50 spectrofluorimeter. The fluorescence lifetimes (uncertainty ±5%) were obtained with an Edinburgh single-photon counting apparatus, in which the flash lamp was filled with D_2. Luminescence quantum yields (uncertainty ±15%) were determined using quinine sulphate in 0.5 M H_2SO_4 aqueous solution (Φ = 0.546).

Synthesis of ligand 1 and complex 2: Compound **3** was prepared according to procedures described in the literature.[9a]

4,4″-Bispropylsulfanyl-6,6″-dipyren-1-yl-2,2′:6′,2″-terpyridine (1): A solution of *t*BuOK (550 mg, 4.90 mmol) in dry THF (15 mL) was added to a refluxing solution of **3** (594 mg, 1.22 mmol) and **4** (600 mg, 2.45 mmol) in dry THF (20 mL) under argon over a period of 2 h. The solution was stirred overnight at room temperature and then acetic acid (6 mL) and NH_4OAc (4 g) were added to the reaction. The mixture was refluxed for 90 minutes, cooled, poured into water (100 mL), extracted with chloroform (3 × 100 mL), washed with saturated aqueous $NaHCO_3$ (100 mL) and dried with Na_2SO_4. After evaporation of the solvent, the crude material was purified by means of flash chromatography (alumina/chloroform) to give **1** (373 mg, 38.9%). ^{1}H NMR ($CDCl_3$): δ = 8.66 (d, J = 1.7 Hz, 2H; H3), 8.62 (d, J = 7.8 Hz, 2H; H2), 8.57 (d, J = 9.3 Hz, 2H; H7′), 8.29 (d, J = 0.9 Hz, 2H; H6), 8.20–8.25 (m, 6H; H7, H9), 8.10–8.15 (m, 6H; H5, H8, H10), 7.90 (t, J = 7.8 Hz, 2H; H1), 7.61 (d, J = 1.7 Hz, 2H; H4), 3.24 (t, J = 7.9 Hz, 8H), 1.88 (sext, J = 7.9 Hz, 8H), 1.21 ppm (t, J = 7.9 Hz, 12H); ^{13}C NMR ($CDCl_3$): δ = 12.9, 24.7, 37.4, 116.1, 119.3, 124.8, 124.9, 126.2, 126.3, 126.6, 127.3, 127.6, 131.7, 138.1, 138.5, 152.9, 157.5, 157.7 ppm; FAB-MS: m/z (%): 783.0 (100) $[M+H]^+$; elemental analysis calcd (%) for $C_{53}H_{39}N_3S_3$ (782.0 g mol^{-1}): C 81.40, H 5.03, N 5.37; found: C 81.75, H 5.26, N 5.10.

Zinc complex 2: Formation from ligand **1** (10 mg, 0.013 mmol), $Zn(OTf)_2$ (4.6 mg, 0.013 mmol), terpy (3 mg, 0.013 mmol) and CD_3CN (0.5 mL) at room temperature. ES-MS: m/z (%): 540.2 (100) $[Zn(\mathbf{1})(terpy)]^{2+}$, 1229.38 (20) $[Zn(\mathbf{1})(terpy)OTf]^+$.

X-ray crystallographic data for 1 and 2: Single crystals of $[C_{53}H_{39}N_3S_2{\cdot}2H_2O]$ (**1**) were grown from an acetonitrile/chloroform mixture. Yellow crystals were placed in oil and a single colourless crystal of dimensions 0.16 × 0.08 × 0.02 mm was selected, mounted on a glass fibre and placed in a low-temperature N_2 stream. The unit cell was monoclinic with a space group of $P12_11$; cell dimensions: a = 16.5598(7), b = 7.6555(3), c = 18.508(1) Å, $\alpha = \gamma = 90°$, β = 108.524(5)°, V = 2224.8(2) Å^3 and Z = 2 (M_r = 860, ρ = 1.22 g cm^{-3}); reflections were collected from $2.5° \le \theta \le 27.41°$ for a total of 8995 of which 2160 were unique with $I > 3\sigma(I)$; number of parameters was 254; final R factors were R_1 = 0.100 (based on observed data), wR_2 = 0.127 (based on all data); GoF = 1.065; maximal residual electron density was 1.110 e Å^{-3}.

Single crystals of $[C_{68}H_{50}N_6S_2Zn{\cdot}2CF_3O_3S{\cdot}2CH_3NO_2]$ (**2**) were grown from an isopropyl ether/nitromethane mixture. Yellow crystals were placed in oil and a single colourless crystal of dimensions 0.15 × 0.06 × 0.04 mm was selected, mounted on a glass fibre and placed in a low-temperature N_2 stream. The unit cell was monoclinic with a space group of $C12/c1$; cell dimensions: a = 56.459(2), b = 13.6160(5), c = 18.9766(7) Å, $\alpha = \gamma = 90°$, β = 99.8(3)°, V = 14374.6(8) Å^3 and Z = 8 (M_r = 6176, ρ = 1.39 g cm^{-3}); reflections were collected from $2.5° \le \theta \le 28.26°$ for a total of 16620 of which 6635 were unique with $I > 2\sigma(I)$; number of parameters was 849; final R factors were R_1 = 0.130 (for $I/\sigma > 4$), wR_2 = 0.170 (based on all data); GoF = 1.390; maximal residual electron density was 1.218 e Å^{-3}.

X-ray diffraction data for **1** and **2** were collected on a Nonius Kappa charge-coupled device (CCD) diffractometer with graphite monochromatised $Mo_{K\alpha}$ radiation (λ = 0.71073 Å), φ scan mode to 173°, at the Laboratoire de Cristallochimie, Université Louis Pasteur, Strasbourg. The structures of **1** and **2** were determined by using direct methods and were refined (based on F^2 using all independent data) by full-matrix least-square methods (SHELXTL 97). Hydrogen atoms were included at calculated positions by using a riding model.

CCDC-227041 (**1**) and CCDC-227042 (**2**) contain the supplementary crystallographic data for this paper. These data can be obtained free of charge via www.ccdc.cam.ac.uk/conts/retrieving.html (or from the Cambridge Crystallographic Data Centre, 12 Union Road, Cambridge CB2 1EZ, UK; fax: (+44) 1223-336-033; or e-mail: deposit@ccdc.cam.ac.uk).

[1] a) J.-M. Lehn, *Supramolecular Chemistry-Concepts and Perspectives*, VCH, Weinheim, **1995**, Chapter 8; b) J.-M Lehn, *Proc. Natl. Acad. Sci. USA* **2002**, *99*, 4763–4768; c) J.-M. Lehn in *Supramolecular Science: Where It Is and Where It Is Going*, (Eds.: R. Ungaro, E. Dalcanale), Kluwer, Dordrecht, **1999**, pp. 287–304.

[2] a) V. Balzani, F. Credi, M. Raymo, J. F. Stoddart, *Angew. Chem.* **2000**, *112*, 3484–3530; *Angew. Chem. Int. Ed.* **2000**, *39*, 3348–3391; b) *Acc. Chem. Res.* **2001**, *34*, Molecular Machines Special Issue; c) *Molecular Switches* (Ed.: B. Feringa), Wiley-VCH, Weinheim, **2001**; ref. [1a], pp. 124–138; e) For an early example of a photoin-

duced process, see: S. Shinkai, T. Nakaji, T. Ogawa, K. Shigematsu, O. Manabe, *J. Am. Chem. Soc.* **1981**, *103*, 111–115.
[3] a) M. Barboiu, J.-M. Lehn, *Proc. Natl. Acad. Sci. USA* **2002**, *99*, 5201–5206; b) M. Barboiu, G. Vaughan, N. Kyritsakas, J.-M. Lehn, *Chem. Eur. J.* **2003**, *9*, 763–769.
[4] S. L. Gilat, S. H. Kawai, J.-M. Lehn, *Chem. Eur. J.* **1995**, *1*, 275–284.
[5] a) C. Mao, W. Sun, Z. Shen, N. C. Seeman, *Nature* **1999**, *397*, 144–146; C. M. Niemeyer, M. Adler, *Angew. Chem.* **2002**, *114*, 3933–3937; *Angew. Chem. Int. Ed.* **2002**, *41*, 3779–3783; b) A recent report describes a proton-fuelled process: D. Liu, S. Balasubramanian, *Angew. Chem.* **2003**, *115*, 5912–5914; *Angew. Chem. Int. Ed.* **2003**, *42*, 5734–5736; c) S. Tyagi, F. R. Kramer, *Nat. Biotechnol.* **1996**, *14*, 303–308.
[6] M. Büschel, M. Helldobler, J. Daub, *Chem. Commun.* **2002**, 1338–1339.
[7] a) J. P. Schneider, J. W. Kelly, *J. Am. Chem. Soc.* **1995**, *117*, 2533–2546; b) P. B. Glover, P. R. Ashton, L. J. Childs, A. Rodger, M. Kercher, R. M. Williams, L. De Cola, Z. Pikramenou, *J. Am. Chem. Soc.* **2003**, *125*, 9918–9919; A. Petitjean, R. Khoury, J.-M. Lehn, *J. Am. Chem. Soc.* **2004**, *126*, in press; d) For bispyrene-appended benzene and pyridine groups, see: H. M. Colquhoun, Z. Zhu, D. J. Williams, *Org. Lett.* **2003**, *5*, 4353–4356.
[8] S. T. Howard, *J. Am. Chem. Soc.* **1996**, *118*, 10269–10274.
[9] a) K. T. Potts, *Bull. Soc. Chim. Belg.* **1990**, *99*, 741–768; b) K. T. Potts, K. A. Gheysen Raiford, M. Keshavarz-K, *J. Am. Chem. Soc.* **1993**, *115*, 2793–2807.
[10] G. Albano, V. Balzani, E. C. Constable, M. Maestri, D. R. Smith, *Inorg. Chim. Acta* **1998**, *277*, 225–231.
[11] L. Prodi, R. Ballardini, M. T. Gandolfi, R. Roversi, *J. Photochem. Photobiol. A* **2000**, *136*, 49–52.
[12] A. Credi, V. Balzani, S. Campagna, G. S. Hanan, C. R. Arana, J.-M. Lehn, *Chem. Phys. Lett.* **1995**, *243*, 102–107.
[13] F. Loiseau, C. Di Pietro, S. Serroni, S. Campagna, A. Licciardello, A. Manfredi, G. Pozzi, S. Quici, *Inorg. Chem.* **2001**, *40*, 6901–6909.
[14] A. Harriman, A. Khatyr, R. Ziessel, *J. Chem. Soc. Dalton Trans.* **2003**, 2061–2068.
[15] In acetonitrile the typical band of ligand **1** can also be observed. However, in the spectra of the complex this band shows a reduced intensity (<2% with respect to the intensity of the free ligand), but at the same time shows an unquenched excited-state lifetime and a corrected excitation spectrum that is proportional to that of the ligand. These findings are a clear indication that such a signal is due to the small portion of the ligand in the solvent that is not complexed. In dichloromethane, in which the association is stronger, the contribution of this band is almost negligible.
[16] a) J. W. Canary, J. Xu, J. M. Castagnetto, D. Rentzeperis, L. A. Marky, *J. Am. Chem. Soc.* **1995**, *117*, 11545–11547; the p*K*a values of tren are 10.43, 9.87 and 9.01 in aqueous solution at 25°C; b) The 1:1 complex of tren with Zn^{2+} has the stability contant $\log K_s = 15.2$; G. Anderegg, V. Gramlich, *Helv. Chim. Acta* **1994**, *77*, 685–690.
[17] The p*K*a values of terpyridine (4.33, 2.64; see R. B. Martin, J. A. Lissfelt, *J. Am. Chem. Soc.* **1956**, *78*, 938–940) are much lower than those of tren (ref. [16b]), so that only the latter is protonated, but not ligand **1**. NMR titration experiments showed a progressive protonation of lateral pyridines of ligand **1** and no subsequent protonation events were observed on addition of a large excess of triflic acid. These spectra are totally different from those of complex **2** and the peaks of protonated species $\mathbf{1}H^+$ and $\mathbf{1}H_2^{2+}$ are not observed during the NMR switching experiments. We also note that the absorption and emission spectra of complex **2** are identical to those obtained in the switching experiments.

Received: December 19, 2003

Published online: April 28, 2004

